

# Fuel Effects on Gas Turbine Combustion-Liner Temperature, Pattern Factor, and Pollutant Emissions

A H Lefebvre\*

Purdue University, West Lafayette, Indiana

An analytical study is made of the substantial body of experimental data acquired during recent Wright Patterson Aero Propulsion Laboratory sponsored programs on the effects of fuel properties on the performance and reliability of several gas turbine combustors, including J79-17A, J79 17C (Smokeless), F101, TF41, TF39, J85, TF33, and F100. Quantitative relationships are derived between certain key aspects of combustion, notably liner wall temperature, pattern factor, and exhaust emissions, and the relevant fuel properties, combustor design features and combustor operating conditions. It is concluded that fuel chemistry, as indicated by hydrogen content and/or aromatics content, has a significant effect on flame radiation and liner wall temperature, but only a slight effect on the emissions of carbon monoxide (CO) and oxides of nitrogen ( $\text{NO}_x$ ). The physical properties that govern atomization quality and evaporation rates affect CO emissions, but other important performance parameters, such as  $\text{NO}_x$  emissions and liner wall temperature, are sensibly independent of physical properties over the range of fuels studied.

## Nomenclature

$A$	= area, $\text{m}^2$
$C_1$	= heat flux from combustion gases to liner wall by convection, $\text{W}/\text{m}^2$
$C_2$	= heat flux from liner wall to annulus air by convection, $\text{W}/\text{m}^2$
$c_p$	= specific heat at constant pressure, $\text{J}/\text{kg K}$
$C/H$	= carbon/hydrogen ratio of fuel, by mass
$D_h$	= hydraulic mean diameter of atomizer air duct at exit plane, $\text{m}$
$D_L$	= liner diameter or height, $\text{m}$
$D_p$	= atomizer prefilmer diameter, $\text{m}$
$f_{pz}$	= fraction of total combustor air employed in primary zone combustion
$k$	= thermal conductivity, $\text{J}/\text{ms K}$
$L$	= length, or luminosity factor
$L_e$	= liner length employed in fuel evaporation, $\text{m}$
$L_L$	= total liner length, $\text{m}$
$l_b$	= mean beam length of radiation path, $\text{m}$
$m$	= mass flow rate, $\text{kg}/\text{s}$
$n$	= reaction order
$P$	= pressure, $\text{Pa}$
$q$	= fuel/air ratio
$q_{ov}$	= combustor overall fuel/air ratio
$q_{ref}$	= reference dynamic head, $\text{kPa}$
$R_1$	= radiation heat flux from combustion gases to liner wall, $\text{W}/\text{m}^2$
$R_2$	= radiation heat flux from liner to casing, $\text{W}/\text{m}^2$
$SMD$	= Sauter mean diameter of fuel spray, $\text{m}$
$T$	= temperature, $\text{K}$
$T_{bn}$	= boiling temperature at normal atmospheric pressure, $\text{K}$
$T_{L_{\max}}$	= maximum liner wall temperature for given fuel, $\text{K}$
$T_{L0}$	= maximum liner wall temperature for JP4 $\text{K}$
$t_e$	= evaporation time, $\text{s}$
$U$	= velocity, $\text{m}/\text{s}$
$V$	= combustion volume (general), $\text{m}^3$
$V_c$	= total combustion zone volume = predilution zone volume, $\text{m}^3$

$V_e$	= evaporation volume, $\text{m}^3$
$\Delta P$	= pressure differential, $\text{kPa}$
$\Delta T$	= temperature rise, $\text{K}$
$\epsilon$	= emissivity
$\lambda_{\text{eff}}$	= effective value of evaporation constant, $\text{m}^2/\text{s}$
$\mu$	= dynamic viscosity, $\text{kg}/\text{ms}$
$\nu$	= kinematic viscosity, $\text{m}^2/\text{s}$
$\rho$	= density, $\text{kg}/\text{m}^3$
$\sigma$	= Stefan Boltzmann constant ( $5.67 \times 10^{-8} \text{W}/\text{m}^2 \text{ K}^4$ ) or surface tension, $\text{kg}/\text{s}^2$

## Subscripts

$A$	= air
$an$	= annulus value
$F$	= fuel, or formation
$g$	= gas
$L$	= liner value
$pz$	= primary zone value
$w$	= wall value
$3$	= combustor inlet value
$4$	= combustor outlet value

## Introduction

THE alternative fuel sources now being sought and the acceptance of a broader specification for aviation fuels highlight the need for prediction techniques that will allow the impact of any change in fuel specification on hardware durability and combustion performance to be estimated accurately in the combustor design stage. Unfortunately the effect of a change in fuel properties is not constant for all combustors but varies between one combustor and another due to differences in operating conditions and differences in design. For example, the effect of an increase in carbon/hydrogen ratio on liner wall temperature is much greater for combustors featuring fuel-rich primary zones than for combustors in which the primary zone is fuel weak. This is because with rich primary zones most of the heat transferred to the liner wall is by radiation, which is proportional to  $\epsilon T_g^4$ . Thus liner wall temperature is dependent on the flame emissivity,  $\epsilon$ , which, in turn, is dependent on the  $C/H$  ratio of the fuel. With fuel weak primary zones, however, most of the heat transferred to the liner wall is by forced convection. Here the dominant term is the gas temperature  $T_g$  which is fairly insensitive to changes in  $C/H$  ratio. In consequence, quite

large changes in  $C/H$  ratio produce only a slight effect on liner wall temperature.

Another complicating factor is that the various properties and characteristics of petroleum fuels are so closely interrelated that it is virtually impossible to change any one property without affecting many others. However, there are several mitigating factors that help to ease the situation. For example, atomization quality is influenced only by the physical properties of the fuel, namely viscosity, surface tension, and density, all of which are easily measured by standard laboratory techniques. Moreover, it can also be shown that evaporation rates are closely linked to the physical properties of the fuel; for example,  $\rho_F$  provides a useful indication of fuel volatility.

The basic data employed in this investigation were obtained from a number of programs initiated by the U.S. Air Force, Army, Navy and NASA, along with engine manufacturers to determine the effects of anticipated future fuels on existing engines. As a result of these studies, data have become available that yield new and useful insights into fuel property effects on combustion performance. References 1-6 also contain detailed information on all the relevant chemical and physical properties of the fuels employed. These fuels were supplied by the U.S. Air Force for combustion system evaluation. They included a current JP4, a current JP8, five blends of the JP4, five blends of the JP8 and, in some cases, a No. 2 diesel fuel. The blends were intended to achieve three different levels of hydrogen content, i.e., 12, 13, and 14% by mass.

The key chemical and physical properties of the fuels selected are listed in Table 1. Additional information on the distillation characteristics of the test fuels is contained in Fig. 1.

In a recent companion paper<sup>7</sup> attention was focused on the influence of fuel chemistry and physical properties on the combustion efficiency, performance, lightup characteristics, and lean blowout limits of gas turbine combustors. The objective of the present work is to extend the analysis to include the effects of fuel type, fuel spray characteristics, liner dimensions, and combustor operating conditions on liner wall temperature pattern factor, and pollutant emissions.

### Fuel Spray Characteristics

A major drawback to the data contained in Refs. 1-6 is that they contain very little information on fuel spray characteristics; in particular, no measurements were made of mean drop size for any of the combustors employed in the investigation.

In the absence of actual measured values, the mean drop size (SMD) was calculated using one of the following two expressions:

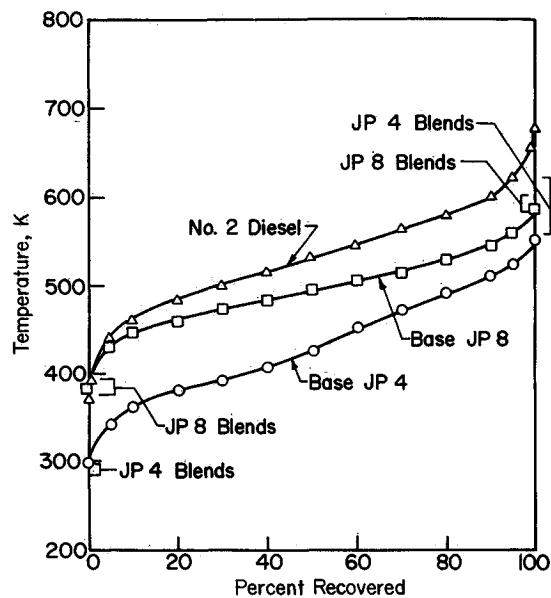


Fig. 1 Distillation characteristics of test fuels<sup>2</sup>

For airblast atomizers<sup>8</sup>

$$\frac{SMD}{D_h} = \left[ 1 + \frac{\dot{m}_F}{\dot{m}_A} \right] \left[ 0.33 \left( \frac{\sigma_F}{\rho_A U_A^2 D_p} \right)^{0.6} \left( \frac{\rho_F}{\rho_A} \right)^{0.1} + 0.068 \left( \frac{\mu_F^2}{\rho_F \sigma_F D_p} \right)^{0.5} \right] \quad (1)$$

For pressure swirl atomizers<sup>9</sup>

$$SMD = 0.071 \sigma_F^{0.25} \nu_F^{0.25} \dot{m}_F^{0.25} \Delta P_F^{0.5} \rho_g^{0.25} \quad (2)$$

Equation (1) takes full account of variations in fuel properties ( $\sigma_F$ ,  $\rho_F$  and  $\mu_F$ ), air properties ( $\rho_A$  and  $U_A$ ), and atomizer geometry ( $D_p$  and  $D_h$ ). The values of the constants and exponents in this equation were established in a number of experimental studies that covered much wider ranges of fuel and air properties than are needed for the present investigation. Thus the main source of error in the use of Eq. (1) stems from uncertainties surrounding the values to be assigned to the atomizer dimensions. With Eq. (2) problems arise in the calculation of  $\rho_g$ , since the primary zone temperature cannot be estimated accurately. Another potentially serious source of error that applies to both equations is that

Table 1 Test fuel chemical and physical properties

Fuel components	Hydrogen contents (H)—weight %	Heating value (net) MJ/kg	Density ( $\rho_{300K}$ ) kg/m <sup>3</sup>	Viscosity ( $\nu_{300K}$ ) mm <sup>2</sup> /s	Surface tension ( $\sigma_{300K}$ ) mN/m	Vapor pressure ( $P_{300K}$ ), kPa
Base fuel	Blending agents					
JP 4	—	14.5	43.603	752.7	0.924	23.27
JP 8	—	14.0	43.210	799.5	1.849	25.85
JP 8	Gulf mineral seal oil	13.9	43.189	801.2	2.071	25.92
JP 8	2040 solvent	12.0	41.947	852.3	1.809	27.62
JP 8	Xylene bottoms	13.0	42.724	813.4	1.428	26.38
JP 8	Xylene bottoms	12.0	42.129	827.6	1.160	26.66
JP 8	2040	13.0	42.556	825.2	1.804	26.42
JP 4	2040	12.0	42.203	829.7	1.141	25.22
JP 4	2040	13.0	42.629	796.3	1.028	23.75
JP 4	Xylene	12.0	42.196	808.0	0.830	25.21
JP 4	Xylene	13.0	42.682	786.5	0.835	24.20
JP 4	Xylene & GMSO	14.0	43.366	769.6	1.057	23.45
2 D	—	13.1	42.691	837.2	3.245	27.35
						1.59

all the experimental work involved in their formulation was carried out under cold, i.e., non burning and fairly quiescent conditions. Clearly, drop sizes could be appreciably different in the true combustor environment due to the combined effects of high temperature, high turbulence, and strong airflow currents.

### Liner Wall Temperature

For the purpose of analysis a liner may be regarded as a container of hot flowing gases surrounded by a casing in which air is flowing between the container and the casing. Broadly the liner is heated by radiation and convection from the hot gases inside it and is cooled by radiation to the outer casing and by convection to the annulus air. The relative proportions of the radiation and convection components depend upon the geometry and operating conditions of the system. Under equilibrium conditions the liner temperature is such that the internal and external heat fluxes at any point are just equal.

$$R_1 + C_1 = R_2 + C_2 \quad (3)$$

#### Internal Radiation, $R_1$

This is the component of heat transfer that is most affected by a change in fuel type. It is given by<sup>10</sup>

$$R_1 = 0.5\sigma(I + \epsilon_w)\epsilon_g T_g^{1.5} (T_g^{2.5} - T_w^{2.5}) \quad (4)$$

The "bulk" or mean gas temperature  $T_g$  is obtained as the sum of the chamber entry temperature  $T_3$  and the temperature rise due to combustion  $\Delta T_{\text{comb}}$ . Thus,

$$T_g = T_3 + \Delta T_{\text{comb}}$$

$\Delta T_{\text{comb}}$  may be derived from standard temperature rise curves. The appropriate value of fuel/air ratio is the product of the local fuel/air ratio and the local level of combustion efficiency. Most heat transfer calculations are carried out at high pressure conditions where it is reasonable to assume a combustion efficiency of 100%.

For the luminous flames associated with the combustion of heterogeneous fuel air mixtures, the value of  $\epsilon_g$  for insertion in Eq. (4) is obtained as<sup>10</sup>

$$\epsilon_g = 1 - \exp - [0.29 P_3 L (q\ell_b)^{0.5} T_g^{-1.5}] \quad (5)$$

where  $q$  is the local fuel/air ratio and  $\ell_b$  is the "beam length" of the radiating gas. Beam length depends on the size and shape of the gas volume. For most practical purposes it is given to sufficient accuracy<sup>10</sup> by the expression

$$\ell_b = 3.4 \text{ (volume/surface area)}$$

The luminosity factor  $L$  is an empirical correction introduced to obtain reasonable agreement between experimental data on gas radiation and predictions from Eq. (4). Experiments have shown that luminosity factor depends largely on the carbon to hydrogen mass ratio of the fuel.<sup>9,10,11</sup>

The original equation for  $L$  is<sup>10</sup>

$$L = 7.53 (C/H - 5.5)^{0.84} \quad (6)$$

Later the following expression was suggested by Kretschmer and Odgers<sup>11</sup>

$$L = 0.0691 [C/H - 1.82]^{2.71} \quad (7)$$

Another correlation, which is simpler and probably no less accurate is<sup>9</sup>

$$L = 3(C/H - 5.2)^{0.75} \quad (8)$$

More recent investigations have tended to emphasize fuel hydrogen content rather than carbon/hydrogen ratio as the property most relevant to flame radiation. Figure 2 shows the correlation obtained by Blazowski and Jackson<sup>12,13</sup> between hydrogen content and liner wall temperature for several engines. The data shown represent cruise conditions with combustor inlet temperatures ranging from 547 to 756 K. The parameter used to correlate the experimental data is

$$(T_{L_{\text{max}}} - T_{L_0}) / (T_{L_0} - T_3)$$

in which the numerator represents the increase in maximum liner temperature over that obtained with a baseline fuel containing 14.5% hydrogen.

The excellent correlation of data exhibited in Fig. 2 could not be duplicated for the results contained in Refs. 1-4 as shown, for example, in Fig. 3. It is believed that this is because the magnitude of the parameter  $(T_{L_{\text{MAX}}} - T_{L_0}) / (T_{L_0} - T_3)$

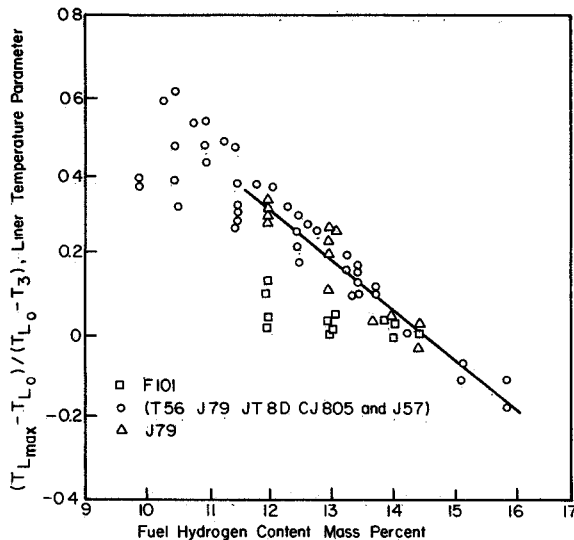


Fig. 2 Effect of fuel hydrogen content on liner temperature parameter at cruise operating conditions.<sup>12,13</sup>

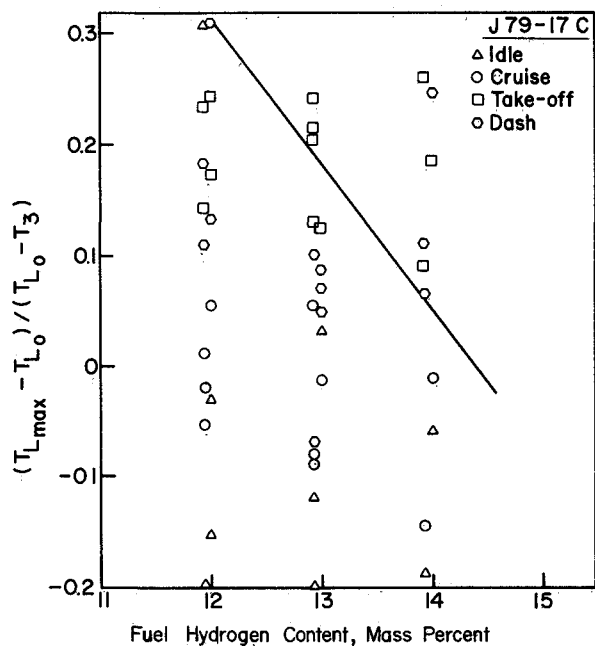


Fig. 3 Effect of fuel hydrogen content on liner temperature parameter for J79 17C combustor

$(T_{L_0} - T_3)$  is very sensitive to the value of  $T_{L_0}$ . Since maximum values of wall temperature are notoriously difficult to determine, this would appear to be a serious drawback to the use of this type of temperature parameter.

An alternative approach attempted here was to find a relationship between fuel hydrogen content and luminosity factor. Analysis of the experimental data led to the following expression

$$L = 336 / (\%H_2)^2 \quad (9)$$

Substitution of this value of  $L$  into Eq. (5) allows calculations of flame radiation to be carried out for all fuels over the entire range of test conditions.

#### External Radiation, $R_2$

The significance of  $R_2$  increases with liner wall temperature, and at low values it can often be neglected. It can be estimated only approximately due to lack of accurate knowledge of wall emissivities. For this reason it is sufficient to use the cooling air temperature  $T_3$  in place of the unknown temperature of the outer air casing.

Values of emissivity for various materials may be obtained from McAdams.<sup>14</sup> However, for most practical purposes the following expression, based on typical values of emissivity and diameter ratio, will suffice<sup>9,10</sup>

$$R_2 = 0.4 \sigma (T_w^4 - T_3^4) \quad (10)$$

#### Internal Convection, $C_1$

Of the four heat transfer processes which together determine the liner temperature, this component is the most difficult to estimate accurately. In the primary zone the gases involved are at high temperature and undergoing rapid physical and chemical change. Further difficulty is introduced by the existence within the primary zone of steep gradients of temperature, velocity, and composition. Uncertainties regarding the airflow pattern, the state of the boundary layer development, and the effective gas temperature make the choice of a realistic model almost arbitrary.

In the absence of more exact data it is reasonable to assume that some form of the classical heat transfer relation for straight pipes will hold for conditions inside a liner, using a Reynolds number index consistent with established practice for conditions of extreme turbulence. This leads to an expression of the form<sup>10</sup>

$$C_1 = 0.017 \left( \frac{k_g}{D_{av}^{0.2}} \right) \left( \frac{\dot{m}_{pz}}{A_L \mu_g} \right)^{0.8} (T_g - T_w) \quad (11)$$

#### External Convection, $C_2$

This is obtained as<sup>10</sup>

$$C_2 = 0.020 \left( \frac{k_A}{D_{an}^{0.2}} \right) \left( \frac{\dot{m}_{an}}{A_{an} \mu_A} \right)^{0.8} (T_w - T_3) \quad (12)$$

The fluid properties are evaluated at the annulus air temperature  $T_3$ . In practice the cooling air temperature increases during the passage downstream, but normally this amounts to no more than a few degrees and can reasonably be neglected.

Restating Eq. (3), for equilibrium

$$R_1 + C_1 = R_2 + C_2$$

Solution of this equation yields the wall temperature,  $T_w$ .

The value of  $T_w$  as determined by the method outlined above represents the liner wall temperature that would be obtained in the absence of internal wall cooling. Unfortunately, Refs. 1-6 do not contain the detailed information

needed to estimate film cooling effects on  $T_w$ . Bearing in mind the lengthy and tedious nature of the procedure involved, it was thus decided to calculate 'uncooled' wall temperatures for four combustors only to ascertain if the results obtained reflected anticipated trends in regard to the effect of fuel hydrogen content on liner wall temperature. The results of these calculations for the J79 17C and F101 combustors are shown in Figs. 4 and 5 for all fuels as plots of  $T_w$  vs hydrogen content.

It may be noted in Figs. 4 and 5 that the calculated values of  $T_w$  are generally higher than the corresponding measured

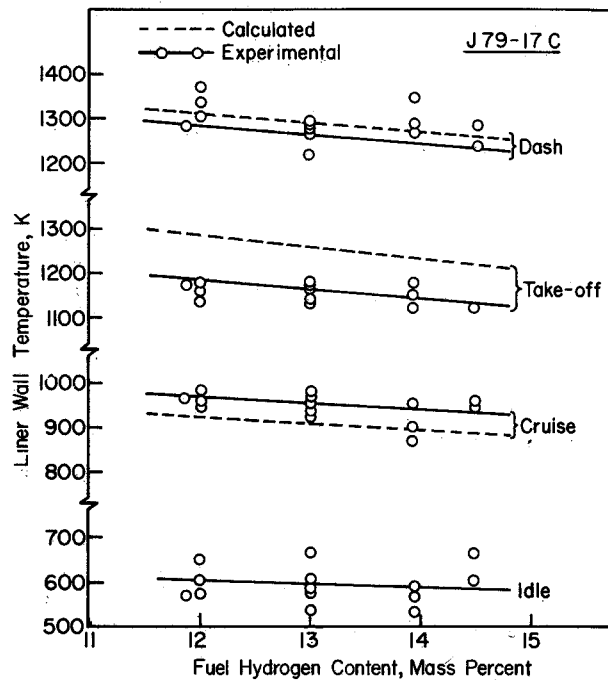


Fig. 4 Comparison of measured and predicted values on the effect of H<sub>2</sub> content on liner temperature for J79 17C combustor

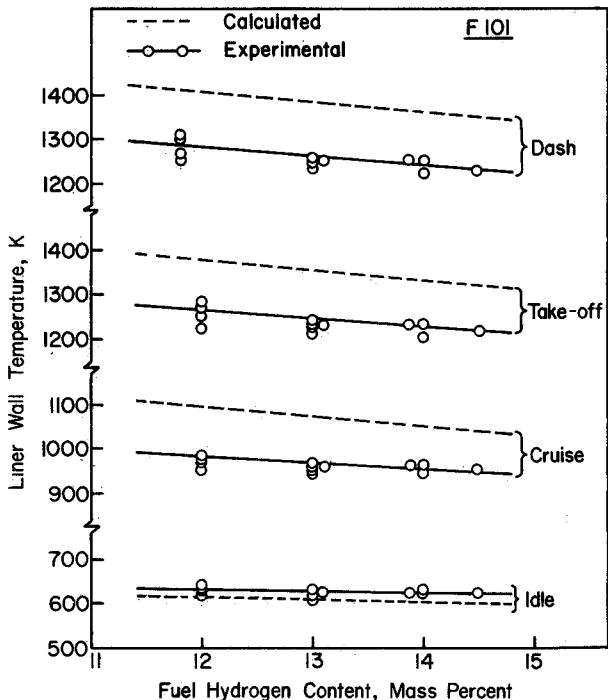


Fig. 5 Comparison of measured and predicted values on the effect of H<sub>2</sub> content on liner temperature for F101 combustor

values due to neglect of internal wall cooling. Only at low power conditions, where the errors incurred through neglect of internal wall cooling are partially balanced by the assumption of 100% combustion efficiency in the combustion zone, do the measured and calculated wall temperatures roughly coincide.

These factors are not considered too serious in a study that is mainly concerned with fuel type because they apply with equal force to all fuels. The fact that the measured and calculated values of  $T_w$  follow the same trend, as evidenced by Figs. 4 and 5, tends to support the validity of using the luminosity factor concept as a convenient means of incorporating fuel hydrogen content into the "standard" equation for flame emissivity. Thus Eq. (5) may be rewritten as

$$\epsilon_g = 1 - \exp - [97.44 P_3 (\%H_2)^{-2} (q\ell_b)^{0.5} T_g^{-1.5}] \quad (13)$$

### Pattern Factor

Perhaps the most important and at the same time most difficult problem in the design and development of gas turbine combustion chambers is that of achieving a satisfactory and consistent distribution of temperature in the efflux gases discharging into the turbine. In the past experience has played a major role in the determination of dilution zone geometry and trial and error methods have been widely used in developing the temperature traverse quality of individual combustor designs to a satisfactory standard. Experimental investigations into dilution zone performance carried out on actual chambers have provided useful guidance but very often it has proved difficult or impossible to distinguish the separate influences of all the variables involved. Thus although it is now generally accepted that a satisfactory temperature profile is dependent upon adequate penetration of the dilution jets coupled with the correct number of jets to form sufficient localized mixing regions, the manner in which the total dilution hole area is utilized in terms of number and size of holes is still largely a matter of experience.

The final mixing process is affected in a complicated manner by the dimensions, geometry, and pressure drop of the liner; the size, shape and discharge coefficients of the liner holes; the airflow distribution to various zones of the chamber; and the temperature distribution of the hot gases entering the dilution zone. For any given combustor, the latter is strongly influenced by fuel spray characteristics such as drop size, spray angle, and spray penetration, since these control the pattern of burning and hence the distribution of temperature in the primary zone efflux. It is known that spray characteristics are strongly influenced by pressure, especially with atomizers of the simplex or dual orifice type, and it is to be expected, therefore, that temperature traverse will also vary with pressure, although the extent of this variation will vary from one chamber to another depending on design and in particular on length.

Several parameters have been proposed to describe the temperature distribution in the combustor efflux. Perhaps the most widely used is the "overall temperature distribution factor" which tends to highlight the maximum temperature found in the traverse and is, therefore, of special importance to the design and durability of nozzle guide vanes. It is normally defined as

$$\text{Pattern factor} = (T_{\max} - T_4) / (T_4 - T_3) \quad (14)$$

### Correlation of Data

Two parameters of crucial importance to pattern factor are liner length which controls the time and distance that are available for mixing, and the pressure drop across the liner which governs the penetration of the dilution jets and their rate of mixing with the products of combustion. In a previous analysis of experimental data on tubular tubo annular and

annular combustors, it was found that<sup>9</sup>

$$(T_{\max} - T_4) / (T_4 - T_3) = \int (L_L / D_L) (\Delta P_L / q_{\text{ref}}) \quad (15)$$

The data correlation obtained for tubular liners is shown in Fig. 6. In connection with this figure it should be noted that the correlation is based not on the  $L/D$  ratio of the dilution zone, but on that of the complete liner. This was found to provide a better fit to the data.

For tubular and tubo annular combustors we have<sup>9</sup>

$$\begin{aligned} (T_{\max} - T_4) / (T_4 - T_3) \\ = 1 - \exp - \left[ 0.070 (L_L / D_L) (\Delta P_L / q_{\text{ref}}) \right]^{-1} \end{aligned} \quad (16)$$

while for annular combustors

$$\begin{aligned} (T_{\max} - T_4) / (T_4 - T_3) \\ = 1 - \exp - \left[ 0.050 (L_L / D_L) (\Delta P_L / q_{\text{ref}}) \right]^{-1} \end{aligned} \quad (17)$$

Since no information on liner pressure loss factor is contained in Refs. 1-6, this might appear to rule out the use of Eqs. (16) and (17) in the present analysis. Another drawback to these equations is the inherent assumption that all the liner length is utilized in mixing and combustion while the length occupied by evaporation processes is essentially zero. Although this assumption is not unreasonable for highly volatile fuels of low viscosity such as JP4, it is difficult to justify for some of the alternative fuels employed in this program. These deficiencies may be remedied by rewriting Eqs. (16) and (17) in the following form, where  $Z=0.07$  or  $0.05$  for tubular and annular liners respectively.

$$\begin{aligned} (T_{\max} - T_4) / (T_4 - T_3) \\ = 1 - \exp - \left[ Z (\Delta P_L / q_{\text{ref}}) / (L_L - L_e) / (D_L) \right]^{-1} \end{aligned} \quad (18)$$

$L_e$  is the liner length required to evaporate the fuel spray. It is obtained as the product of the average predilution liner velocity and the evaporation time, as is shown in Eq. 19

$$L_e = U_g t_e = \left( \frac{0.6 \dot{m}_A}{\rho_g A_L} \right) \left( \frac{D_o^2}{\lambda_{\text{eff}}} \right) \quad (19)$$

The constant of 0.6 in Eq. (19) stems from the assumption that 60% of the total combustor airflow enters the liner upstream of the dilution zone. A more accurate assessment of this constant for each individual liner design would not be justified at this stage due to the larger uncertainty surrounding the value of  $D_o$ . In practice it was found that correlation of experimental data could be improved by reducing the value of this constant from 0.6 to 0.33. This may be explained on the grounds that the combustion process does not wait until the fuel has fully evaporated; instead burning commences as soon as sufficient fuel has evaporated to produce a flammable mixture. Thus Eq. (18) may be rewritten as

$$\begin{aligned} \frac{T_{\max} - T_4}{T_4 - T_3} \\ = 1 - \exp - \left[ Z \left( \frac{\Delta P_L}{q_{\text{ref}}} \right) \left( \frac{L_L}{D_L} - \frac{0.33 \dot{m}_A D_o^2}{\rho_g A_L D_L \lambda_{\text{eff}}} \right) \right]^{-1} \end{aligned} \quad (20)$$

where  $\rho_g$  is the average gas density upstream of the dilution

zone. It is calculated at a temperature  $T_g$  which is obtained as

$$T_g = T_3 + \Delta T_g$$

where  $\Delta T_g$  is the temperature rise due to combustion for a fuel/air ratio of 0.6,  $q_{ov}$ ,  $A_L$  is the average cross sectional area of the liner. It is estimated by dividing the volume of the liner by its maximum length,  $D_L$ , is the average diameter or height of the liner. For a tubular liner it is readily obtained as  $D_L = (4A_L/\pi)^{0.5}$ .

Mean drop sizes for insertion into Eq. (20) were calculated using either Eq. (1) or Eq. (2). Values of  $\lambda_{eff}$  were read off the graphs of  $\lambda_{eff}$  vs  $T_{bn}$  contained in Ref. 15, using values for  $T_{bn}$  obtained from Refs. 16 at fuel temperatures corresponding to the average boiling point (50% recovered).

For the three tubular combustors examined (namely, the J79-17A, J79-17C, and TF41), values of  $Z(\Delta P_L/q_{ref})$  of 0.99, 1.03, and 1.17, respectively, provided excellent correlations of the experimental data, as illustrated in Figs. 7 and 8. Reference to Eq. (16) shows that these values of  $Z(\Delta P_L/q_{ref})$  correspond to liner pressure loss factors for these combustors of 14, 15, and 17, respectively. It is of interest to note that the improvement in pattern factor with increase in engine power (due to reduction in evaporation time, as predicted by Eq. (20)), is fully borne out by the results contained in Figs. 7 and 8.

The influence of fuel type on pattern factor is manifested through the effects of mean drop size (via viscosity and surface tension) and effective evaporation constant (via  $T_{bn}$ ) on droplet evaporation time. Over the range of fuels examined the effect of fuel type on pattern factor is relatively small, at least at high power conditions where the evaporation time is always a small fraction of the total combustor time, regardless of fuel type. However, if measurements of pattern

factor are conducted at operating conditions where the evaporation time constitutes a significant proportion of the total residence time, then a strong effect of fuel type on pattern factor should be expected. This, in fact, was precisely the result obtained with the F101 combustor when the effect of fuel type on pattern factor was examined at various simulated engine operating conditions using air supplied at normal atmospheric pressure. The results of these tests are shown in Fig. 9, where it is of interest to note that the measured values of pattern factor are well correlated by Eq. (20) using a value for  $Z(\Delta P_L/q_{ref})$  of 2.0. Figure 9 demonstrates a clear effect of fuel type on pattern factor, but it would be erroneous to assume that these data have any relevance to the real engine. If Eq. (20) is used to calculate values of pattern factor at actual takeoff conditions (including  $P_f$ ), it is found that pattern factor is virtually in

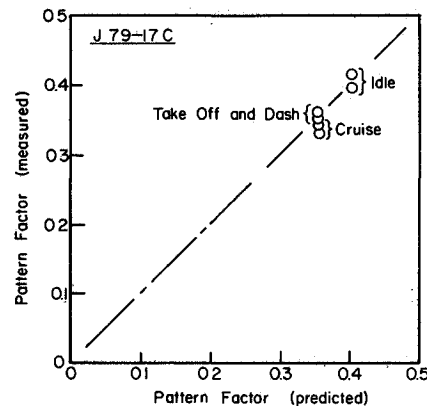


Fig. 8 Comparison of measured and predicted values of pattern factor for J79-17C combustor

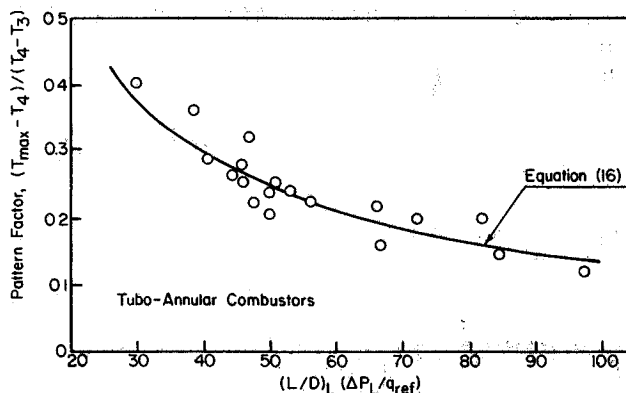


Fig. 6 Pattern factor correlation for tubo-annular combustors

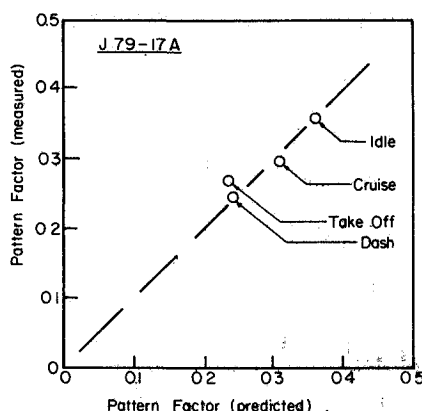


Fig. 7 Comparison of measured and predicted values of pattern factor for J79-17A combustor.

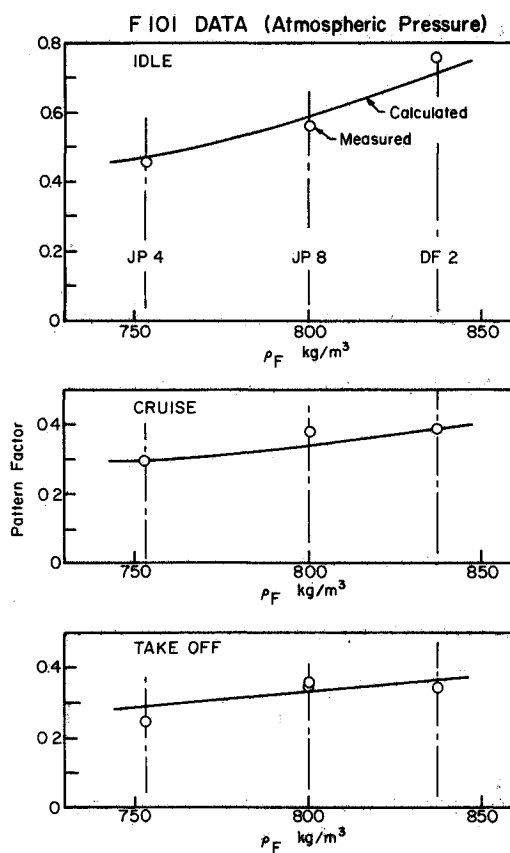


Fig. 9 Comparison of measured and predicted values of pattern factor for F101 combustor

dependent of fuel type, as shown in Fig. 10. Thus from a practical viewpoint, the results of the F101 tests are fully consistent with those of all other combustors. They all confirm that at the high power conditions where pattern factor is most important to engine durability variation in fuel type has a negligible effect.

### Pollutant Emissions

In recent years several papers and reports have been issued on the accomplishments made in the reduction of pollutant emissions from gas turbine combustors (see for example, Refs. 16-19). Most modeling of emission characteristics has been concerned with oxides of nitrogen,  $\text{NO}_x$ , but efforts have also been made to predict the formation of other important pollutant species. To be successful, a model must accommodate the complex flow behavior and include a kinetic scheme of the important chemical reactions occurring within the combustor. The kinetics of some relevant combustion processes are, unfortunately, not well understood at the present time, particularly for the production of carbon, carbon monoxide, and the hydrocarbon species that are intermediaries in the fuel oxidation process.

The primary requirement for a satisfactory emissions model for gas turbine combustors is that it should represent an optimum balance between accuracy of representation, utility, ease of use, economy of operation and capability for further improvement. In recent years considerable efforts have been directed toward the development of relatively complex mathematical emissions models that can be applied to gas turbines. They have varied in level of sophistication from those with potential to yield a complete description of the relevant thermodynamic and chemical properties as a function of spatial location within the combustor, to others which merely assume that homogeneous conditions exist at all axial stations.<sup>20,28</sup>

The high cost and complexity of the more sophisticated mathematical models have encouraged the development of semi empirical models for  $\text{NO}_x$  and CO emissions. Hung's approach to the modeling of  $\text{NO}_x$  emissions places more emphasis on the physical processes considered to be important and relegates chemical kinetics to a relatively minor role.<sup>29</sup> His analysis includes a five region combustor internal flowfield model, fuel distribution models for liquid and gaseous fuels, a single overall hydrocarbon complete combustion model, a nitric oxide formation model based on the Zeldovich mechanism, a diffusion limited complete mixing model, and a model to account for the influence of ambient humidity. This model has been used successfully in

predicting the influence on  $\text{NO}_x$  emissions of water injection and wide variations in fuel type.<sup>29,32</sup>

Other successful semi empirical models for predicting emissions have been developed by Fletcher and Heywood<sup>20,33</sup> and by Hammond and Mellor.<sup>34,36</sup> Useful critical evaluations of both mathematical and semi empirical prediction methods have been made by Rubins and Marchionna,<sup>37</sup> Sullivan and Mas,<sup>38</sup> and Odgers.<sup>39</sup>

Empirical models can also play an important role in the design and development of low emission combustors. They may serve to reduce the complex problems associated with emissions to forms which are more meaningful and tractable to the combustion engineer, who often requires only an insight and a quick estimate of the levels attainable with the design variables at his disposal. They also permit more accurate correlations of emissions for any one specific combustor than can be achieved by the more general analytical models discussed previously.

In attempting to derive an empirical model for emissions emphasis is placed on  $\text{NO}_x$  and CO. This is because the highly complex and unknown nature of the hydrocarbon oxidation reaction makes it virtually impossible to derive a satisfactory model for unburned hydrocarbons. Attempts to correlate soot data have met with some success in regard to the prediction of exhaust smoke levels, but have failed to account properly for the effects of aromatics/hydrogen content on soot formation and smoke.<sup>40</sup>

For both nitric oxide and carbon monoxide it may be assumed that their exhaust concentration is proportional to the product of three terms which are selected to represent the following: 1) mean residence time in the combustion zone, 2) chemical reaction rates, and 3) mixing rates.

Expressions for these three parameters may be derived in simplified form as is now shown.

Residence time =  $L/U = L\rho A/\dot{m}_A = PV/(\dot{m}_A RT)$  [i.e., residence time  $\propto (PV/(\dot{m}_A T))$ ] It is assumed that reaction rates are a function of pressure and temperature only, i.e. reaction rate  $\propto P^m \exp(zT)$  for  $\text{NO}_x$  and reaction rate  $\propto P^n \exp(cT)$  for CO. It is assumed that mixing rates are a function of liner pressure drop. Specifically we have mixing rate  $\propto (\Delta P/P)^x$ . Thus  $\text{NO}_x = f(\text{residence time})(\text{reaction rate})(\text{mixing rate})$  or

$$\begin{aligned} \text{NO}_x &= A \left( \frac{PV}{\dot{m}_A T} \right) \left( \frac{\Delta P}{P} \right)^x P^m \exp(zT) \\ &= \frac{AV_c (\Delta P/P)^x P^y \exp(zT)}{\dot{m}_A T} \end{aligned} \quad (21)$$

where  $y = 1 + m$ , and  $A$  is a constant.

Similarly, for CO we have  $\text{CO} = f(\text{residence time})^{-1} (\text{reaction rate})(\text{mixing rate})$  or

$$\begin{aligned} \text{CO} &= C \left( \frac{\dot{m}_A T}{PV_c} \right) \left( \frac{\Delta P}{P} \right)^a P^n \exp(-cT) \\ &= C V_c^{-1} \dot{m}_A T (\Delta P/P)^a P^b \exp(-cT) \end{aligned} \quad (22)$$

where  $b = n - 1$  and  $C$  is a constant.

It is recognized that the above equations have no strong theoretical foundation. However, they do embody the main variables of combustor size, pressure loss, flow proportions and operating conditions of inlet pressure, temperature and air mass flow. The effect of variations in overall combustor fuel/air ratio is also included via its influence on primary zone temperature. Fuel type affects both flame temperature and mean drop size. For  $\text{NO}_x$ , drop size is unimportant since at the high pressure conditions where  $\text{NO}_x$  emissions are most

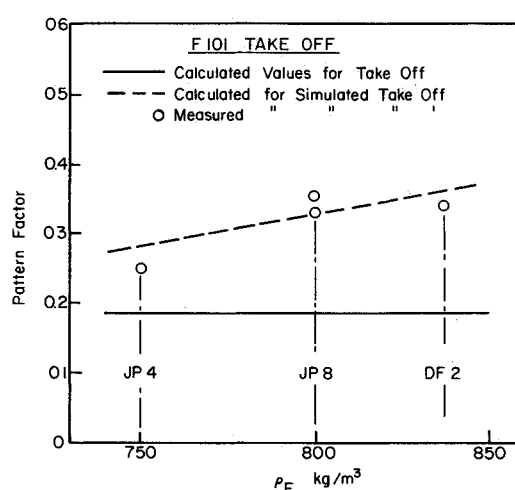


Fig. 10 Graphs illustrating the effects of fuel density and combustor operating conditions on pattern factor

prominent, the fraction of the total combustion volume employed in fuel evaporation is so small that wide variations in fuel drop size have a negligible effect on  $\text{NO}_x$  emissions. However at low pressure operation where CO emissions attain their highest concentrations, a significant proportion of the primary zone volume is needed to evaporate the fuel. Under these conditions, any factor that influences fuel evaporation rates such as evaporation constant or mean drop size will have a direct effect on the volume available for chemical reaction and therefore, on the emissions of CO and UHC. Thus for the correlation of CO data, the effects of fuel type cannot be ignored. The manner in which they may be introduced conveniently into the equation for CO emissions is illustrated below. From analysis of the experimental data contained in Refs 1-6 it was found for Eq. (21) that  $A = 9 \times 10^{-8}$ ,  $x = 0.125$  and  $z = 0.01$ . For Eq. (22) the results show that  $C = 86$ ,  $a = -0.5$ ,  $b = -1.5$  and  $c = 0.00345$ .

Substituting these values into Eqs. (21) and (22) gives

$$\text{NO}_x = \frac{9 \times 10^{-8} P_3^{1.25} V_c \exp(0.01 T_{st})}{\dot{m}_A T_{pz}} \text{ g/kg} \quad (23)$$

$$\text{CO} = \frac{86 \dot{m}_A T_{pz} \exp(-0.00345 T_{pz})}{\left( V_c - 0.55 \frac{f_{pz} \dot{m}_A D_0^2}{\rho_{pz} \lambda_{\text{eff}}} \left( \frac{\Delta P_L}{P_3} \right)^{0.5} P_3^{1.5} \right)} \text{ g/kg} \quad (24)$$

From Eq. (23) it may be noted that the only influence of fuel type on  $\text{NO}_x$  formation is via the two temperature terms  $T_{pz}$  and  $T_{st}$ . The former is calculated as

$$T_{pz} = T_3 + \Delta T_{pz}$$

where  $\Delta T_{pz}$  is the temperature rise due to combustion corresponding to the inlet temperature  $T_3$  and fuel/air ratio ( $q_{0v}/f_{pz}$ ).  $T_{st}$  is the stoichiometric flame temperature corresponding to the inlet temperature  $T_3$ . Equation (23) suggests that in the combustion of heterogeneous fuel air mixtures it is the stoichiometric flame temperature that determines the formation of  $\text{NO}_x$ . However, for the residence time in the combustion zone which is also significant to  $\text{NO}_x$  formation the appropriate temperature term is the bulk value  $T_{pz}$ , as indicated in the denominator of Eq. (23).

Equation (23) is suitable for conventional spray combustors only. For lean premix/prevaporize combustors in which the maximum attainable temperature is  $T_{pz}$ , it may still be used, provided that  $T_{pz}$  is substituted for  $T_{st}$ . It should also be noted that predictions of  $\text{NO}_x$  based on Eq. (23) tend to be too high when the overall combustor air/fuel ratio exceeds a value of around 100. This is because with diminishing fuel/air ratio the flame shrinks back toward the fuel nozzle and no longer occupies the entire combustion volume  $V_c$ . However, this is not considered a serious drawback since in practice interest is normally focused on conditions of high fuel/air ratio where  $\text{NO}_x$  formation rates attain their highest values.

The excellent correlation of experimental data on  $\text{NO}_x$  provided by Eq. (23) is illustrated in Figs 11-15. Equally good correlations have been demonstrated for all other combustors except the J85 for which the measured values are too low to correlate.<sup>40</sup>

The formation of CO in the primary combustion zone takes appreciably longer than the time required to produce  $\text{NO}_x$ . In consequence the relevant temperature is not the local peak value adjacent to the evaporating fuel drops but the average value throughout the primary zone namely  $T_{pz}$ . Also because CO emissions are most important at low pressure conditions where evaporation rates are relatively slow, it is necessary to reduce the combustion volume  $V_c$  by the volume occupied in fuel evaporation  $V_e$ . This was evaluated

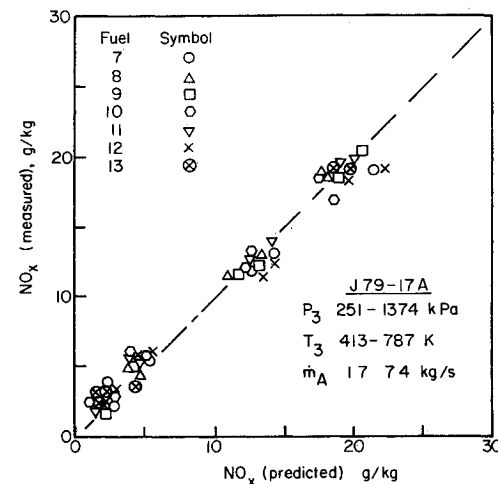


Fig. 11 Comparison of measured and predicted values of  $\text{NO}_x$  emissions for J79 17A combustor (fuels 7 to 13)

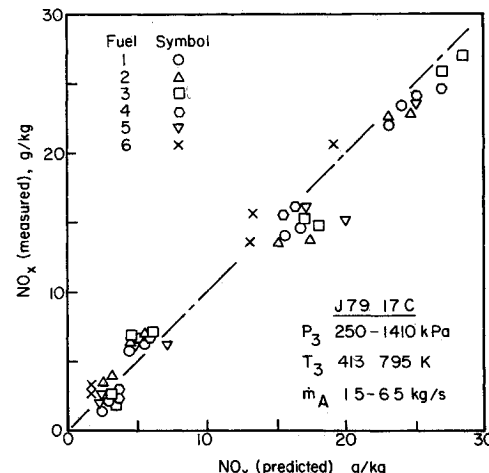


Fig. 12 Comparison of measured and predicted values of  $\text{NO}_x$  emissions for J79 17C combustor (fuels 1 to 6)

elsewhere<sup>7</sup> as

$$V_e = 0.55 f_{pz} \dot{m}_A D_0^2 / \rho_{pz} \lambda_{\text{eff}} \quad (25)$$

It is of interest to note the inclusion of a pressure loss term in Eq. (24). This suggests that the higher turbulence created by an increase in liner pressure drop promotes better mixing in the combustion zone and helps to eliminate the rich and weak pockets of fuel/air mixture, both of which are conducive to high rates of CO formation.

The very satisfactory correlation of experimental data on CO emissions obtained with Eq. (24) is illustrated in Figs 16-20 for J79 17A, J79 17C, F101, TF41, and F100 combustors, respectively.

## Discussion and Summary

### Liner Wall Temperature

The most important factor governing liner wall temperature is the combustor inlet temperature  $T_3$ . Inlet pressure is also significant due to its influence on the concentration of soot particles in the flame, and hence on the magnitude of the luminous radiation flux to the liner wall. At maximum power conditions where liner wall temperatures are of most concern evaporation rates are so high that the physical properties of the fuel appear to have a negligible influence on  $T_w$ . Chemical affects are also quite small as shown in Figs 4 and 5. However, even small increases in maximum values of liner wall temperature can seriously curtail liner life. Thus for the

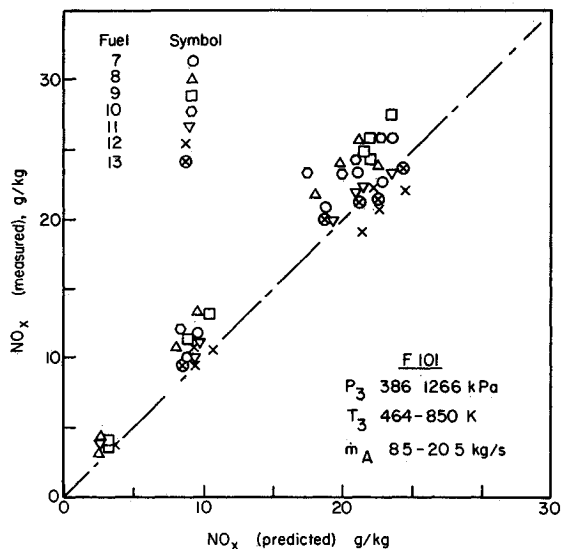


Fig. 13 Comparison of measured and predicted values of  $\text{NO}_x$  emissions for F101 combustor (fuels 7 to 13)

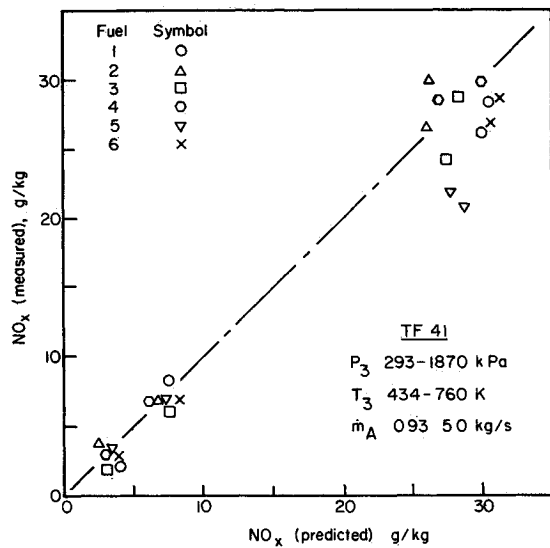


Fig. 14 Comparison of measured and predicted values of  $\text{NO}_x$  emissions for TF 41 combustor (fuels 1 to 6)

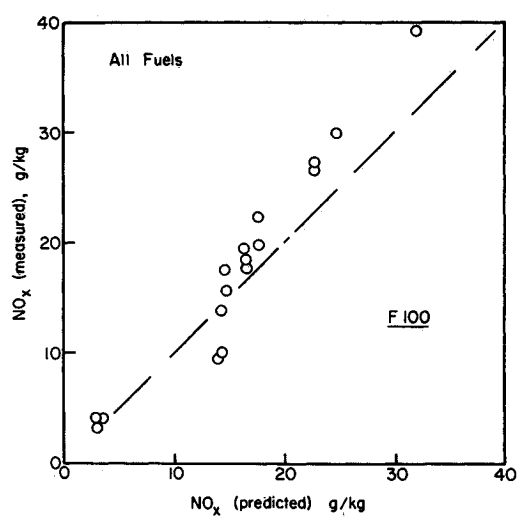


Fig. 15 Comparison of measured and predicted values of  $\text{NO}_x$  emissions for F100 combustor

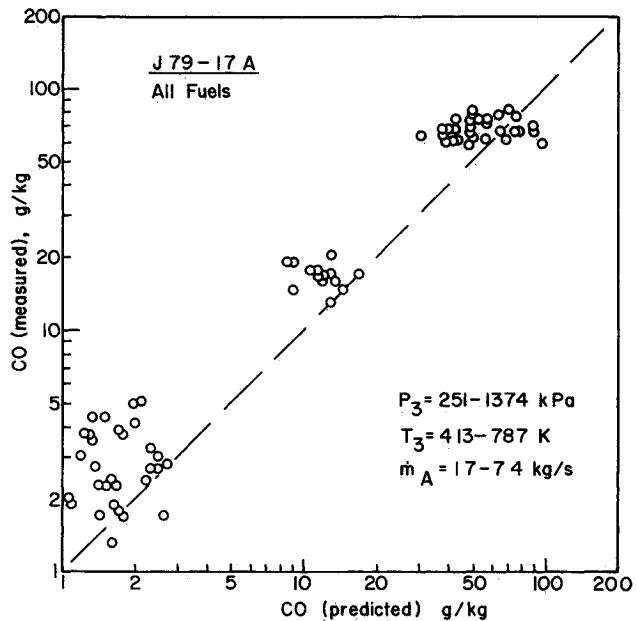


Fig. 16 Comparison of measured and predicted values of CO emissions for J79-17A

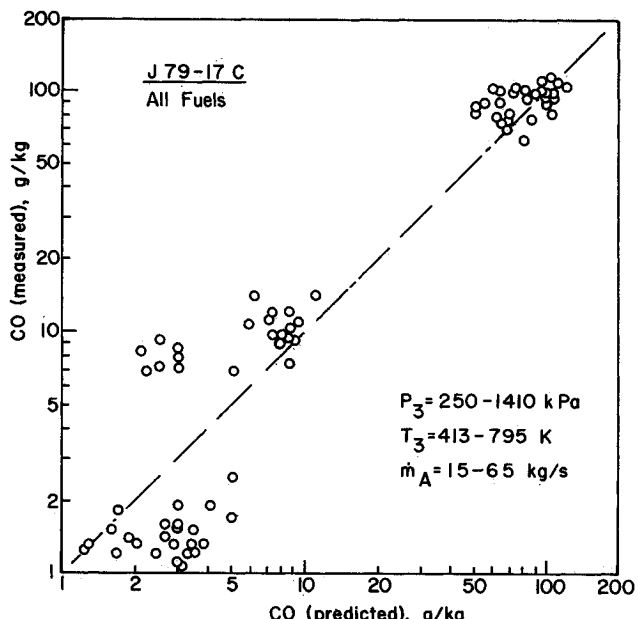


Fig. 17 Comparison of measured and predicted values of CO emissions for J79-17C combustor

range of fuels covered in this investigation, fuel type must be considered important to liner durability

In the calculation of liner wall temperatures, the effect of fuel type can be accommodated quite conveniently by introducing the fuel hydrogen content into the existing equation for gas emissivity. This approach leads to the following equation for  $\epsilon_g$  shown previously as Eq. (13)

$$\epsilon_g = 1 - \exp - [97.44 P_3 (\%H_2)^{-2} (q \ell_b)^{0.5} T_g^{-1.5}]$$

#### Pattern Factor

This is described with good accuracy by Eq. (20)

$$\frac{T_{\max} - T_4}{T_4 - T_3}$$

$$= 1 - \exp - \left[ Z \left( \frac{\Delta P_L}{q_{\text{ref}}} \right) \left( \frac{L_L}{D_L} - \frac{0.33 \dot{m}_A D_o^2}{\rho_g A_L D_L \lambda_{\text{eff}}} \right) \right]^{-1}$$

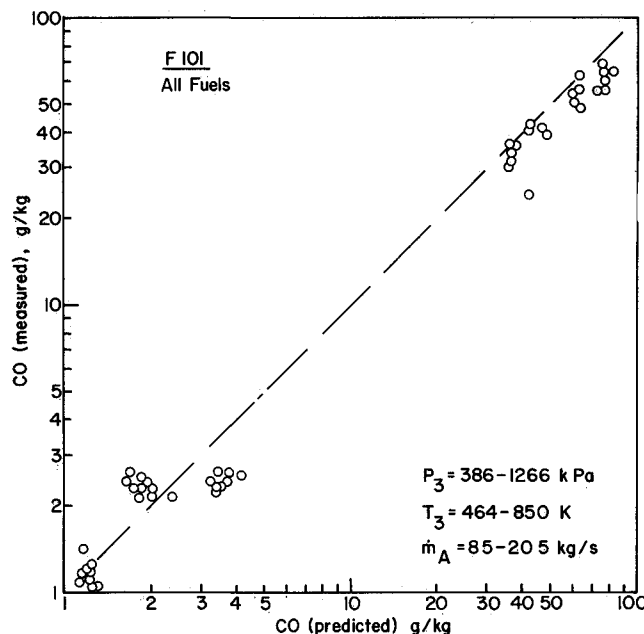


Fig 18 Comparison of measured and predicted values of CO emissions for F101 combustor

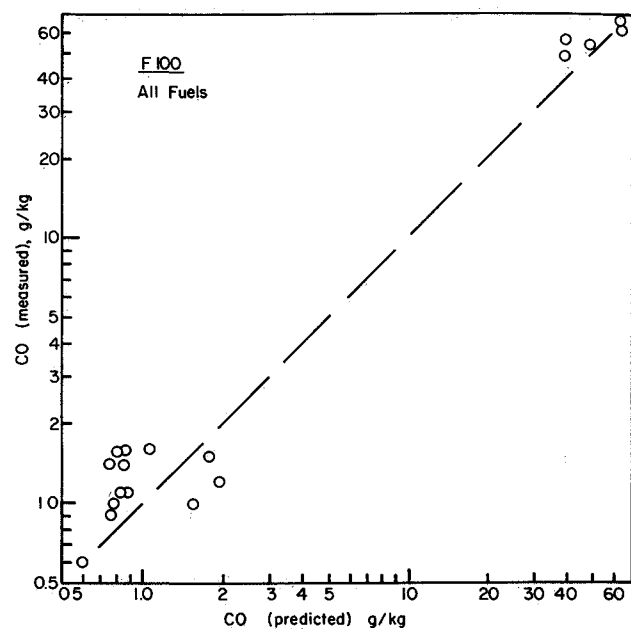


Fig 20 Comparison of measured and predicted values of CO emissions for F100 combustor

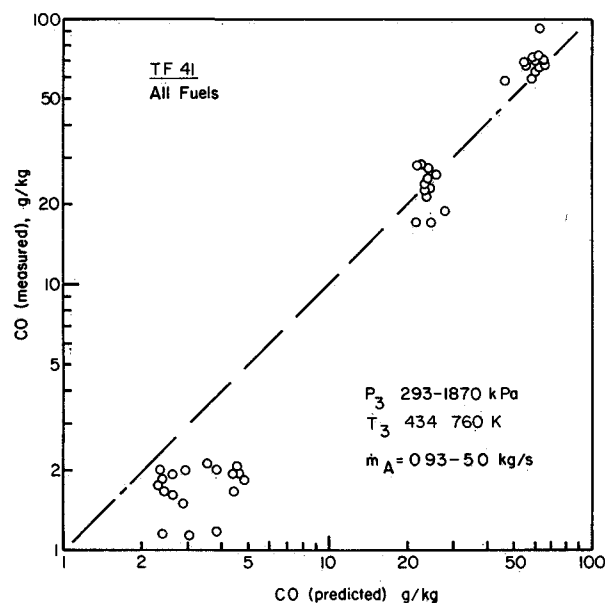


Fig 19 Comparison of measured and predicted values of CO emissions for TF 41 combustor

where appropriate values of  $Z$  are 0.70 and 0.50 for tubo annular and annular combustors, respectively. The above equation shows that the two main parameters controlling pattern factor are the pressure drop across the liner and the liner  $L/D$  ratio. It also accounts for the influence of evaporation time in reducing the time available for mixing within the liner. At the high pressure conditions where pattern factor is of most concern, the evaporation time is always quite short in comparison to the total residence time of the combustor and so the dependence of pattern factor on fuel type is fairly small, as illustrated in Fig 10.

With reduction in engine power, the evaporation time increases due to increase in  $D_o$  and reduction in  $\lambda_{eff}$ . This produces a deterioration in pattern factor as indicated by Eq (20) and also by Figs 7-9, which demonstrate that pattern factor at idle is distinctly worse than at takeoff for all engines. These considerations highlight the importance of measuring

pattern factor only at the correct combustor inlet conditions of  $m_A$ ,  $P_3$ ,  $T_3$  and  $q_{ov}$  corresponding to engine operation at maximum power. Tests carried out at simulated conditions at lower pressure levels give misleading results, as shown in Fig 9. First, they yield values that are overoptimistic and second, they show a dependence of pattern factor on fuel type which greatly exaggerates the dependence actually observed at high pressure.

#### NO<sub>x</sub> Emissions

It is found that NO<sub>x</sub> emissions are very dependent on combustor operating conditions, and also on the size of the combustion zone which governs the time available for NO<sub>x</sub> formation. The key factor controlling NO<sub>x</sub> is the stoichiometric flame temperature which in turn is almost solely dependent on combustor inlet temperature. As far as fuel type is concerned physical properties are of little consequence, except at low power conditions where NO<sub>x</sub> emissions are always quite small due to the corresponding low values of  $T_{st}$ . Fuel chemistry also has little influence on NO<sub>x</sub> because it affects only slightly the values of bulk gas temperature ( $T_{pz}$ ) and stoichiometric flame temperature ( $T_{st}$ ) in the following equation for NO<sub>x</sub>, Eq 23

$$NO_x = \frac{9 \times 10^{-8} P_3^{1/25} V_c \exp(-0.01 T_{st})}{m_A T_{pz}} \text{ g/kg}$$

#### CO Emissions

These are correlated by Eq 24:

$$CO = \frac{86 m_A T_{pz} \exp(-0.00345 T_{pz})}{\left( V_c - 0.55 \frac{f_{pz} m_A D_o^2}{\rho_{pz}} \right) \left( \frac{\Delta P_L}{P_3} \right)^{0.5} P_3^{1/5}} \text{ g/kg}$$

It is again observed that combustor size and operating conditions play a prominent role in determining the level of CO emissions. Special importance is attached to inlet temperature and primary-zone fuel/air ratio, due to their combined effect in resolving the primary zone temperature. As in the case of NO<sub>x</sub> emissions the influence of fuel chemistry is small and is manifested through slight variations

in  $T_{pz}$  with changes in lower calorific value. However since CO emissions attain their maximum values at low power conditions, where a sizeable proportion of the total residence time in the combustion zone is occupied by evaporation processes, the influence of those physical properties that affect evaporation rates, namely  $\mu_F$ ,  $\sigma_F$  and  $T_{bn}$ , becomes important. On this basis it would be anticipated that fuels of high viscosity would be characterized by slightly higher levels of CO emissions, and the experimental data generally confirm this expectation.

### Conclusions

1) Analysis of the experimental data, which cover a wide range of fuel types from JP4 to DF2, shows that fuel chemistry, as indicated by hydrogen content and/or aromatics content, has a significant effect on flame radiation and liner wall temperature.

2) The influence of fuel chemistry on CO and  $\text{NO}_x$  emissions is quite small and stems from the effects of slight differences in lower calorific value on combustion temperature.

3) The physical properties that govern atomization quality and evaporation rates affect CO emissions but, at high power conditions, both liner wall temperature and  $\text{NO}_x$  emissions are sensibly independent of physical properties over the range of fuels studied.

4) Fuel chemistry has no direct influence on pattern factor. However, physical properties have an effect that is appreciable at lower power conditions but that diminishes in importance with increase in engine power, becoming very small at the highest power setting where the effect of pattern factor on vane life is most significant.

### Acknowledgments

Support of the work reported here by the Fuels Branch of the Air Force Aero Propulsion Laboratory, Wright Patterson Air Force Base Ohio, is gratefully acknowledged. The Air Force Technical Monitors employed on this program were Dr Thomas A Jackson in the initial phase, and Mr Curtis M Reeves for the remainder of the program.

### References

- 1 Gleason, C C, Oller T L, Shayeson M W and Bahr D W, 'Evaluation of Fuel Character Effects on J79 Engine Combustion System' AFAPL-TR-79 2015 June 1979
- 2 Gleason C C, Oller T L, Shayeson M W, and Bahr D W, 'Evaluation of Fuel Character Effects on F101 Engine Combustion System' AFAPL TR-79 2018 June 1979.
- 3 Vogel R E, Troth D L and Verdouw A J, 'Fuel Character Effects on Current, High Pressure Ratio Can Type Turbine Combustion Systems,' AFAPL TR 79 2072 April 1980
- 4 Gleason C C, Oller, T L, Shayeson, M W and Kenworthy, M J, 'Evaluation of Fuel Character Effects on J79 Smokeless Combustor,' AFWAL-TR 80 2092, Nov 1980
- 5 Oller T L, Gleason C C, Kenworthy, M. J, Cohen J D, and Bahr, D W, 'Fuel Mainburner/Turbine Effects' AFWAL TR 81 2100, May 1982
- 6 Russel P. L., Fuel Mainburner/Turbine Effects 'AFWAL TR 81 2081, Sept 1982
- 7 Lefebvre, A H, 'Fuel Effects on Gas Turbine Combustion—Ignition Stability and Combustion Efficiency' to be published in *Transactions of the ASME Journal of Engineering for Power*
- 8 Lefebvre A H, 'Airblast Atomization' *Progress in Energy Combustion Science* Vol 6, 1980 pp 231 261.
- 9 Lefebvre A H, *Gas Turbine Combustion* McGraw Hill Book Co., 1983
- 10 Lefebvre A H and Herbert M W, 'Heat Transfer Processes in Gas Turbine Combustion Chambers' *Proceedings of the Institution of Mechanical Engineers* Vol 174 No 12 1960, pp 463 473
- 11 Kretschmer, D and Odgers J, 'A Simple Method for the Prediction of Wall Temperatures in a Gas Turbine Combustor' *ASME Paper No 78 GT-90* 1978
- 12 Blazowski W S, 'Combustion Considerations for Future Jet Fuels' *Sixteenth Symposium (International) on Combustion* The Combustion Institute, 1977, pp 1631 1638
- 13 Jackson, T A, 'Fuel Character Effects on the J79 and F101 Engine Combustion Systems' *Symposium on Aircraft Research and Technology for Future Fuels*, NASA Lewis Research Center 1980
- 14 McAdams W H, *Heat Transmission* 3rd ed McGraw Hill Book Co., New York 1954 Chap 4
- 15 Lefebvre A H and Chin J S, 'Effective Values of Evaporation Constant for Hydrocarbon Fuel Drops' *Proceedings of 20th Automotive Technology Development Contractors Meeting* P 120 1982 pp. 325 331
- 16 Jones, R E and Grobman, J, 'Design and Evaluation of Combustors for Reducing Aircraft Engine Pollution' *Atmospheric Pollution by Aircraft Engines* AGARD CP 125 1973
- 17 Bahr, D W, 'Technology for the Reduction of Aircraft Turbine Engine Exhaust Emissions' *Atmospheric Pollution by Aircraft Engines* AGARD CP 125, 1973
- 18 Henderson R E and Blazowski W S, 'Aircraft Gas Turbine Pollutant Limitations Oriented Toward Minimum Effect on Engine Performance' *Atmospheric Pollution by Aircraft Engines* AGARD CP-125, 1973.
- 19 Jones R E, Diehl L A, Petrush D A and Grobman J, 'Results and Status of the NASA Aircraft Engine Emission Reduction Technology Program' NASA TM 79009, 1978.
- 20 Fletcher, R S. and Heywood, J B, 'A Model for Nitric Oxide Emissions from Aircraft Gas Turbine Engines' AIAA Paper 71 123 1971
- 21 Mosier S A and Roberts R, 'Development and Verification of an Analytical Model for Predicting Emissions from Gas Turbine Engine Combustors during Low Power Operation,' AGARD CP 125 1973
- 22 Roberts R, Aceto L D, Kollrack R, Teixeira, D P, and Bonnell J. M, 'An Analytical Model for Nitric Oxide Formation in a Gas Turbine Combustor,' *AIAA Journal* Vol 10 June 1972 pp 820 826
- 23 Mador, R J and Roberts R, 'A Pollutant Emission Prediction Model for Gas Turbine Combustors' AIAA Paper 74 1113, 1974
- 24 Edelman R and Economos C, 'A Mathematical Model for the Jet Engine Combustion Pollutant Emissions,' AIAA Paper 71 714, 1971
- 25 Mongia H G., and Smith K, 'An Empirical/Analytical Design Methodology for Gas Turbine Combustors' AIAA Paper 78 949 1978
- 26 Bruce T. W., Mongia H C, and Reynolds, R S, 'Combustor Design Criteria Evaluation, Vol 1, UASRTL TR 78 55A' 1979
- 27 Swindenbank, J, Turan, A and Felton P G, 'Three Dimensional Two Phase Mathematical Modelling of Gas Turbine Combustors' *Gas Turbine Combustor Design Problems*, Hemisphere 1980 pp 249 314
- 28 Pratt D T, 'Coalescence/Dispersion Modelling of Gas Turbine Combustors' *Gas Turbine Design Problems*, Hemisphere, 1980, pp 315-330.
- 29 Hung W S Y, 'An Experimentally Verified  $\text{NO}_x$  Emission Model for Gas Turbine Combustors' ASME Paper No 75 GT 71 1975
- 30 Hung W S Y, 'Accurate Method of Predicting the Effect of Humidity on Injected Water on  $\text{NO}_x$  Emissions from Industrial Gas Turbines,' ASME Paper No 74 WA/GT 6 1974
- 31 Hung W S Y, 'A Diffusion Limited Model that Accurately Predicts the  $\text{NO}_x$  Emissions from Gas Turbine Combustors Including the Use of Nitrogen Containing Fuels' ASME Paper No 75 Pwr 11 1975
- 32 Hung W S Y, 'Modeling and Measurement of  $\text{NO}_x$  Emissions from Burning Synthetic Coal Gas in Gas Turbine Combustors' ASME Paper No 75 WA/GT 3, 1975
- 33 Fletcher R S, Siegel R D and Bastress E K, 'The Control of Oxides of Nitrogen Emissions from Aircraft Gas Turbine Engines' NREC 1162 FAA RD 71 111 Vols I II and III Northern Research and Engineering Corp Cambridge, Mass 1971
- 34 Hammond, D C Jr and Mellor A M, 'Analytical Calculations for the Performance and Pollutant Emissions of Gas Turbine Combustors' *Combustion Science and Technology* Vol 4 No 3 1971 pp 101 112

<sup>35</sup>Hammond D C Jr and Mellor, A M , 'Analytical Predictions of Emissions from and within an Allison J 33 Combustor ' *Combustion Science and Technology* Vol 6 No 5 1973 pp 279 286

<sup>36</sup>Mellor, A M Semi Empirical Correlations for Gas Turbine Emissions, Ignition and Flame Stabilization *Progress in Energy Combustion Science* Vol 6 1981 pp 347 358

<sup>37</sup>Rubins, P M , and Marchionna N. R , Evaluation of NO<sub>x</sub> Prediction Correlation Equations for Small Gas Turbines *Journal of Aircraft* Vol 15 Aug 1978 pp 497 502

<sup>38</sup>Sullivan D A and Mas P A ' A Critical Review of NO<sub>x</sub> Correlations for Gas Turbine Combustors ASME Paper 75 WA/GT 7 1975

<sup>39</sup>Odgers, J , Current Theories of Combustion within Gas Turbine Chambers, ' *Fifteenth Symposium (International) on Combustion* The Combustion Institute 1975 pp 1321 1338

<sup>40</sup>Lefebvre A H , Fuel Effects on Gas Turbine Combustion AFWAL TR 83 2004 1984

*From the AIAA Progress in Astronautics and Aeronautics Series . . .*

## INJECTION AND MIXING IN TURBULENT FLOW—v. 68

*By Joseph A Schetz Virginia Polytechnic Institute and State University*

Turbulent flows involving injection and mixing occur in many engineering situations and in a variety of natural phenomena. Liquid or gaseous fuel injection in jet and rocket engines is of concern to the aerospace engineer; the mechanical engineer must estimate the mixing zone produced by the injection of condenser cooling water into a waterway; the chemical engineer is interested in process mixers and reactors; the civil engineer is involved with the dispersion of pollutants in the atmosphere; and oceanographers and meteorologists are concerned with mixing of fluid masses on a large scale. These are but a few examples of specific physical cases that are encompassed within the scope of this book. The volume is organized to provide a detailed coverage of both the available experimental data and the theoretical prediction methods in current use. The case of a single jet in a coaxial stream is used as a baseline case and the effects of axial pressure gradient, self propulsion, swirl, two-phase mixtures, three dimensional geometry, transverse injection, buoyancy forces and viscous inviscid interaction are discussed as variations on the baseline case.

200 pp 6 x 9 illus \$17.00 Mem., \$27.00 List

TO ORDER WRITE Publications Dept , AIAA, 1633 Broadway, New York, N Y 10019